JCB Article

High resolution mapping of mast cell membranes reveals primary and secondary domains of FcεRI and LAT

Bridget S. Wilson, Janet R. Pfeiffer, Zurab Surviladze, Elizabeth A. Gaudet, and Janet M. Oliver

Department of Pathology and Cancer Research and Treatment Center, University of New Mexico Health Sciences Center, Albuquerque, NM 87131

In mast cells, cross-linking the high-affinity IgE receptor (FcεRI) initiates the Lyn-mediated phosphorylation of receptor ITAMs, forming phospho-ITAM binding sites for Syk. Previous immunogold labeling of membrane sheets showed that resting FcεRI colocalize loosely with Lyn, whereas cross-linked FcεRI redistribute into specialized domains (osmiophilic patches) that exclude Lyn, accumulate Syk, and are often bordered by coated pits. Here, the distribution of FcεRI β is mapped relative to linker for activation of T cells (LAT), Grb2-binding protein 2 (Gab2), two PLCγ isoforms, and the p85 subunit of phosphatidylinositol 3-kinase (PI3-kinase), all implicated in the remodeling of membrane inositol phospholipids. Before activation, PLCγ1 and Gab2 are not strongly membrane associated, LAT occurs in small membrane clusters separate from receptor, and PLCγ2, that coprecipitates with LAT, occurs in clusters and along cytoskeletal cables. After activation, PLCγ2, Gab2, and a portion of p85 colocalize with FcεRI β in osmiophilic patches. LAT clusters enlarge within 30 s of receptor activation, forming elongated complexes that can intersect osmiophilic patches without mixing. PLCγ1 and another portion of p85 associate preferentially with activated LAT. Supporting multiple distributions of PI3-kinase, FcεRI cross-linking increases PI3-kinase activity in anti-LAT, anti-FcεRIβ, and anti-Gab2 immune complexes. We propose that activated mast cells propagate signals from primary domains organized around FcεRIβ and from secondary domains, including one organized around LAT.

Introduction

In 1972, Singer and Nicolson introduced the fluid mosaic model of membrane structure. Integrating a large body of work, this model proposed that cellular membranes are essentially two-dimensional solutions composed of integral membrane proteins within a lipid matrix. Although this model is still used to describe membrane organization locally, exceptions to the random arrangement of membrane constituents were immediately described, including evidence that leukocyte membrane proteins can segregate into or out of membrane that is internalized during phagocytosis (Tsan and Berlin, 1971; Oliver et al., 1974) and that antibodies and plant lectins can induce the movement of membrane proteins into patches and caps in fibroblasts, lymphocytes, and erythrocytes (for review see Berlin et al., 1974, 1975). Continued work by many investigators made it clear that membrane proteins rarely undergo random diffusion over long distances. Many factors, including cytoskeletal tethers and motors, interactions with both cytoplasmic and matrix proteins, and segregation with membrane lipids into somewhat ordered domains, contribute to their limited and/or directed movement (for review see Jacobson and Dietrich, 1999).

Current interest in organized regions of membrane, variously called microdomains, rafts, detergent-resistant membranes, and glycosylphosphatidylinositol-enriched membranes, centers around their potential roles in signal propagation and membrane trafficking (Edidin, 1997; Simons and Ikonen, 1997; Anderson, 1998; Brown and London, 1998; Jacobson and Dietrich, 1999). Typically, these membranes are isolated by detergent extraction and sucrose gradient centifugation, yielding a light fraction that accumulates acylated Src-family kinase members and is also enriched for glycerophosphatidylinositol-linked proteins, glycosphingolipids, gangliosides, and cholesterol. Detergent-resistant microdomains on leukocyte surfaces are particularly implicated in signaling via multi-chain immune recognition receptors, including the TCR, BCR, several Fcγ receptors, and the high-affinity IgE receptor (FcεRI)* of mast cells and basophils (for reviews see

Address correspondence to Bridget S. Wilson, Department of Pathology, University of New Mexico Health Sciences Center, CRF 205, 2325 Camino de Salud, Albuquerque, NM 87131. Tel.: (505) 272-8852. Fax: (505) 272-1435. E-mail bwilson@salud.unm.edu

Key words: microdomains; PLCγ; phosphatidylinositol 3-kinase; LAT; Gab2

*Abbreviations used in this paper: DNP-BSA, dinitrophenol-conjugated BSA; FcεRI, high-affinity IgE receptor; Gab2, Grb2-binding protein 2; LAT, linker for activation of T cells; PI3-kinase, phosphatidylinositol 3-kinase; PtdIns(3,4,5)P_3, phosphatidylinositol 3,4,5-triphosphate; RBL-2H3, rat basophilic leukemia cell line 2H3.

Horejsi et al., 1999; Langlet et al., 2000; Dráber et al., 2001).

The high-affinity IgE receptor of mast cells and basophils is an $\alpha\beta\gamma_2$ tetramer with immunoreceptor tyrosine-based activation motifs (ITAMs) in both the β and γ subunit cytoplasmic tails. Cross-linking this receptor activates the Src-family kinase, Lyn, initiating a cascade of events that include the activation of Syk, PLCγ and phosphatidylinositol 3-kinase (PI3-kinase), the mobilization of Ca^{2+}, the secretion of inflammatory mediators from granules, the production of Th2 cytokines, and other events including membrane ruffling, spreading and increased adhesive activity. From detergent extraction and sucrose gradient centrifugation studies, Field et al. (1995, 1997, 1999) suggested that cross-linked FcεRI moves into detergent-resistant microdomains to encounter Lyn. Stauffer and Meyer (1997) localized a fluorescent Syk-SH2 domain with aggregated FcεRI in ganglioside-enriched membrane patches. These and other recent experiments using fluorescent reporters (Teruel and Meyer, 2000) have provided new insights into dynamics of signal transduction both temporally and spatially but are limited by the resolution of the light microscope.

Recently, we used immunogold labeling of mast cell membrane sheets and analysis by transmission electron microscopy to document the locations of signaling proteins at higher resolution during FcεRI signaling in rat basophilic leukemia cell line 2H3 (RBL-2H3) mast cells. We showed that the sequential association of FcεRI with Lyn and Syk occurs in topographically distinct microdomains (Wilson et al., 2000). In resting cells, FcεRI are distributed as dispersed small aggregates that are often loosely colocalized with small Lyn aggregates. After cross-linking, FcεRI redistribute to membrane domains that stain more intensely than bulk membrane with osmium. These osmiophilic membrane patches exclude Lyn and recruit Syk. Receptors are ultimately internalized through coated pits that bud from the periphery of the patches.

Here, plasma membrane sheets from RBL-2H3 mast cells are used to map the distribution of FcεRI β in relation to a further subset of proteins in the signaling cascade, including PLCγ1, PLCγ2, and PI3-kinase implicated in the remodeling of membrane inositol phospholipids, as well as the scaffolding/adaptor proteins, linker for activation of T cells (LAT) and Grb2-binding protein 2 (Gab2). Our results suggest that activated mast cells may propagate signals from primary signaling domains organized around FcεRI β and from secondary signaling domains, including one organized around the transmembrane protein, LAT.

Results

Phospholipase Cγ isoforms have distinct distributions in resting and activated mast cells

Previously, we showed that RBL-2H3 cells contain ~10-fold more PLCγ2 than PLCγ1 and that there are substantial differences in the distribution of these PLCγ isoforms in RBL-2H3 cells. In particular, the results of immunoelectron microscopy in LR-White–embedded cells indicated that a portion of PLCγ2 is inherently associated with the plasma membrane, whereas PLCγ1 is recruited to membrane ruffles in response to FcεRI cross-linking (Barker et al., 1998).

These results are confirmed and extended here. As shown in Fig. 1 A, PLCγ2 interacts strongly with the membrane of resting cells. Nevertheless, very little of this enzyme associates with FcεRI β (Fig. 1 A, Table I). Instead, PLCγ2 occurs in resting cells either in small dispersed clusters or along submembranous cables (Fig. 1 A). The cables can be labeled with gold conjugates of antimyosin antibodies (Fig. 2, A and B) and phalloidin (Fig. 2, B and C), identifying them as components of the cortical actomyosin cytoskeleton.

Supporting the microscopic evidence that a portion of PLCγ2 associates directly with the cytoskeleton, we performed coprecipitation studies using detergent-lysed RBL-2H3 cells. Light, intermediate, and heavy fractions from sucrose gradient centrifugation of the Triton X-100 extracts of resting and activated RBL-2H3 cells were used as the starting material for these studies. PLCγ2 and myosin were absent from the lightest fractions of the gradient but were both immunoprecipitated from the intermediate and heavy fractions (data not shown). Coprecipitating proteins in the immune complexes were resolved by SDS-PAGE and immunoblotting. Anti-PLCγ2 immunoprecipitates contained actin; antimyosin immunoprecipitates contained PLCγ2 (Fig. 2 D). These results support an association in both resting and activated cells between PLCγ2 and the cytoskeletal polymers, actin and myosin.

In contrast to PLCγ2, very little PLCγ1, the minor isoform of PLCγ in RBL-2H3 cells, was bound to the membrane of unstimulated mast cells (Fig. 3 A; Table I).

Total numbers of gold particles recognizing PLCγ2 at the plasma membrane did not change after a 2-min activation (Table I), consistent with earlier data obtained by counting anti-PLCγ2 gold label in ultrathin sections prepared from LR-White–embedded cells and analyzed by standard TEM (Barker et al., 1998). Nevertheless, FcεRI cross-linking induced a strong association of PLCγ2 with receptors in osmiophilic patches (Table I; Fig. 1, B and C). Although direct observation (Fig. 1 B) and gold particle counting (data not shown) indicated no significant drop in PLCγ2 along the lengths of cytoskeletal elements after activation, we cannot rule out the possibility that some PLCγ2 recruited to receptor patches may have originated from the cytoskeleton-associated pool.

The distribution of PLCγ1 on membrane sheets from activated cells is shown in Fig. 3 B and quantified in Table I. FcεRI cross-linking doubles the number of PLCγ1-gold particles on membrane sheets. These gold particles occur as singlets and small clusters that are only occasionally seen near FcεRI β or in osmiophilic patches (Fig. 3 B). Wortmannin treatment, shown previously to inhibit PLCγ1 translocation and tyrosine phosphorylation (Barker et al., 1998), reduces the FcεRI-mediated recruitment of PLCγ1 to membrane sheets (Table I).

Distribution of PI3-kinase in activated cells

Maximal PLCγ activation after FcεRI cross-linking is dependent on both tyrosine phosphorylation and on the activation of PI3-kinase to form phosphatidylinositol-3,4,5-P_3 (PtdIns[3,4,5]P_3), implicating D-3 phosphoinositides in deter-

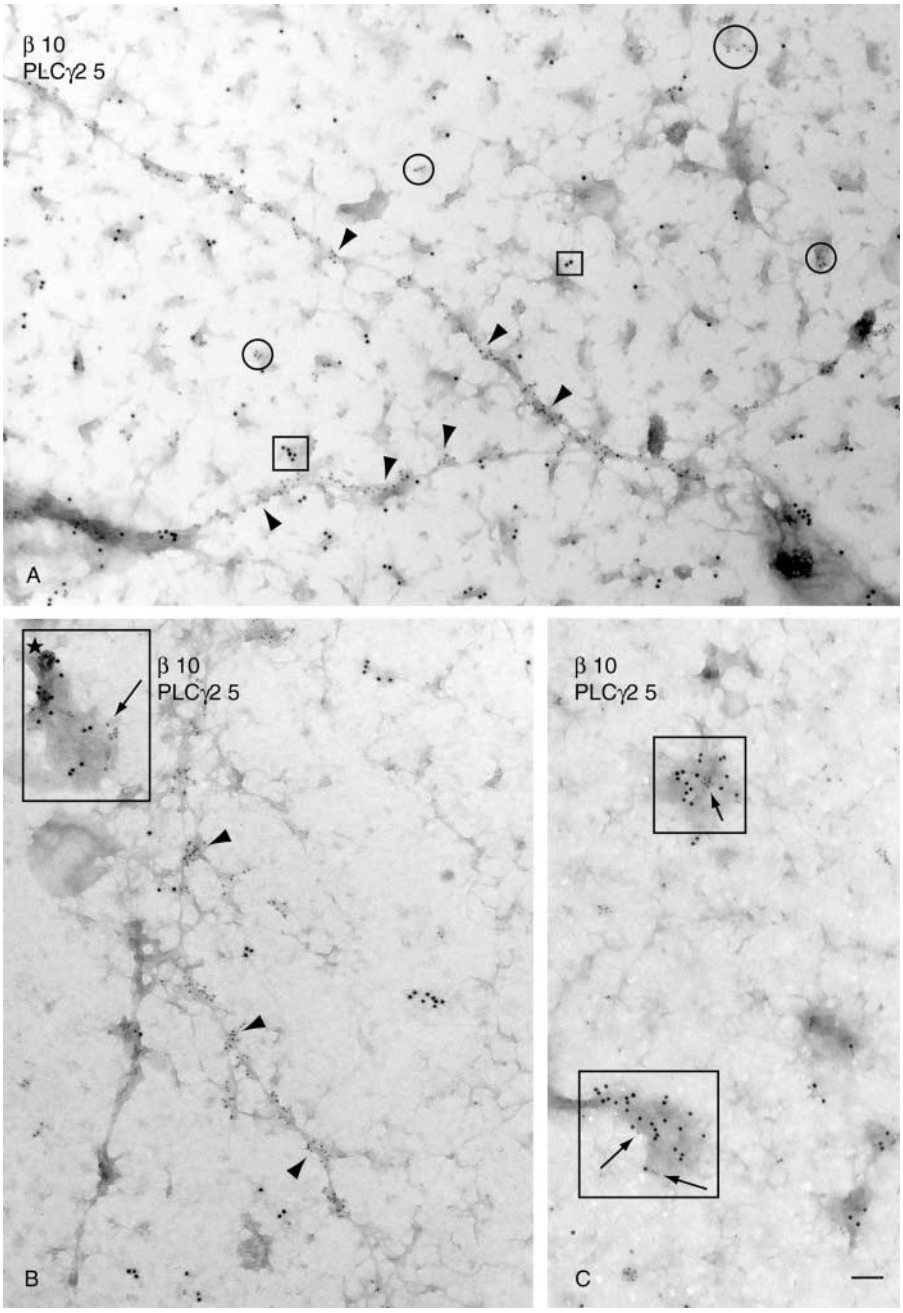

Figure 1. **PLCγ2 redistributes to FcεRI-rich osmiophilic patches in activated mast cells.** Membrane sheets were prepared from RBL-2H3 cells before (A) or after (B and C) cross-linking the FcεRI with DNP-BSA. Sheets were double-labeled with anti-FcεRI β monoclonal antibody conjugated to 10-nm anti–mouse gold particles and anti-PLCγ2 antibody conjugated to 5-nm anti–rabbit gold particles. (A) 10-nm gold particles marking FcεRI are distributed in small clusters and singlets (boxed regions) that do not mix substantially with small clusters of 5-nm gold particles marking PLCγ2 on the membrane (circled regions) and on cytoskeletal cables (arrowheads). (B and C) 5-nm gold particles marking PLCγ2 (arrows) colocalize with 10-nm gold particles specific for FcεRI in osmiophilic membrane patches (boxed regions). *Marks a coated vesicle budding from the patch in B. PLCγ2 label also persists along cytoskeletal cables in activated cells (arrowheads). Bar, 0.1 μm.

Table I. **PLCγ distribution on membrane sheets**

	Resting	2′ XL	Wortmannin + 2′XL
Total PLCγ2 gold particles	2,182	2,215	—
Fold increase PLCγ2 gold particles	—	—	—
% colocalized with FcεRI β gold particles and in osmiophilic patches	6.7%	33.2%	—
Total PLCγ1 gold particles	363	712	514
Fold increase PLCγ1 particles	—	2×	1.4×
% colocalized with FcεRI β gold particles and in osmiophilic patches	6.6%	10.8%	8%

Membrane sheets were prepared from IgE-primed resting or activated (2 min with 0.1 mg/ml DNP-BSA) cells and labeled for PLCγ2 or PLCγ1 and FcεRI β; where indicated, cells were treated with 10 nM Wortmannin before 2-min activation. Numbers of gold particles marking the PLCγ isoforms and their proximity to particles marking FcεRI β were counted for matching areas of membrane for each data set. For PLCγ2, gold particles were counted for 30 μm^2 of membrane; for PLCγ1, gold particles were counted for 97.5 μm^2 of membrane.

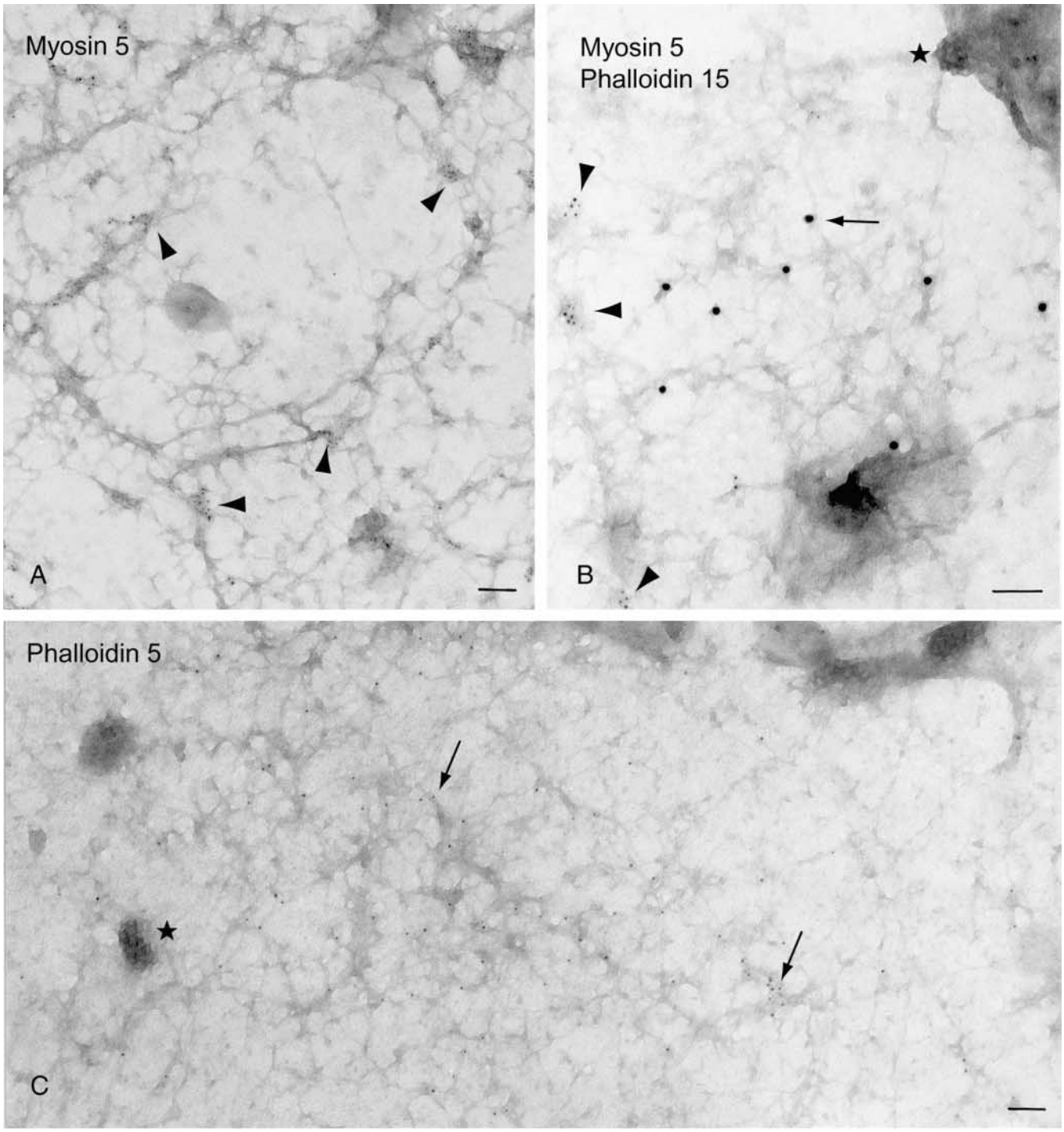
Myosin 5
A
Myosin 5
Phalloidin 15
B
Phalloidin 5
C

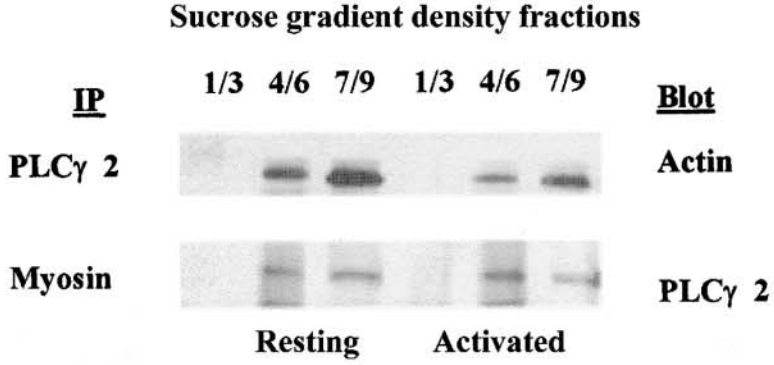
Sucrose gradient density fractions
IP
1/3 4/6 7/9 1/3 4/6 7/9
Blot
PLCγ 2
Actin
Myosin
PLCγ 2
Resting
Activated

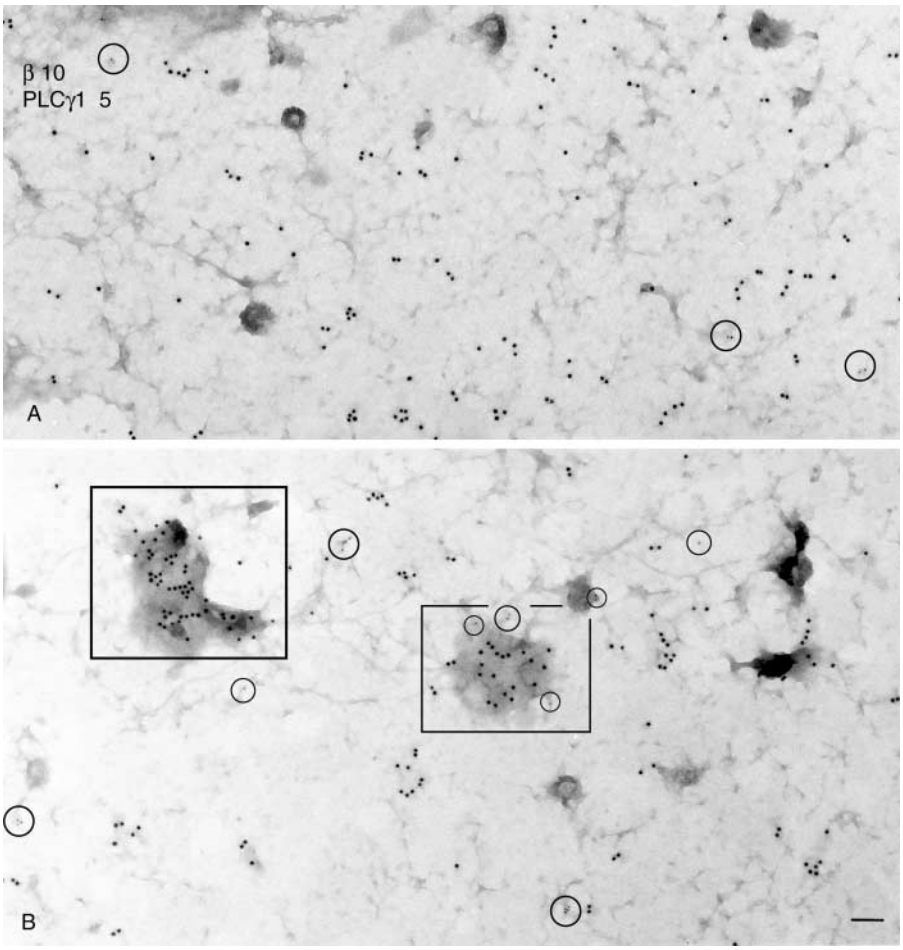

Figure 3. **PLCγ1 membrane label increases after FcεRI activation, mostly outside of osmiophilic patches.** RBL-2H3 membrane sheets were labeled with 5-nm anti-PLCγ1 gold particles and with 10 nm anti-FcεRI β gold particles. In resting cells (A), there are very few 5-nm gold particles marking PLCγ1 (circled regions) and no FcεRI β-PLCγ1 colocalization. In stimulated cells (B), there is an increase in 5-nm gold particles marking PLCγ1 (circled regions), but very few of these particles colocalize with 10-nm gold marking FcεRI in osmiophilic patches (boxed regions). Bar, 0.1 μm.

mining both the location and catalytic activity of tyrosine phosphorylated PLCγ (Barker, et al., 1999; Smith et al., 2001). In Fig. 4, polyclonal antibodies to the noncatalytic p85 subunit were used to localize the heterodimeric class IA PI3-kinases on membrane sheets. The sheets were colabeled with monoclonal antibodies to FcεRI β or to PLCγ isoforms. Fig. 4 A shows the scattered distribution of p85 label on membrane sheets prepared from resting cells. After 2 min of antigen stimulation, a substantial portion of p85 is strongly colocalized with FcεRI in osmiophilic patches (Fig. 4 B, boxed regions).

The p85 subunit of PI3-kinase can be detected in FcεRI immunoprecipitates (see Fig. 10 A); anti-FcεRI β immune complexes from activated cells have ~3× as much PI3-kinase activity as anti-FcεRI β immune complexes from resting cells (Fig. 5 A). The specificity of the assay was confirmed by use of the PI3-kinase inhibitor, Ly294002. Relative to the levels of activity in anti-p85 immunoprecipitates, this represents <5% of total PI3-kinase activity (Fig. 5 D). The results suggest that a small but significant fraction of p85 forms detergent-stable complexes with FcεRI β, which becomes activated after FcεRI phosphorylation and movement into osmiophilic patches.

Clusters of p85 also occur outside the osmiophilic patches (Fig. 4, B and C, circled regions). The micrograph in Fig. 4 C shows that some of the p85 clusters outside of osmiophilic patches colocalize with PLCγ1. Despite this clear association seen by microscopy, we were unable to measure PI3-kinase activity in PLCγ1 immune complexes prepared from detergent lysates of activated RBL-2H3 cells (data not shown). The most plausible explanation, supported by the biochemical studies reported in Barker et al. (1999) and Smith et al. (2001), is that the association seen by microscopy principally reflects the recruitment of PLCγ1-PH to newly synthesized PtdIns(3,4,5)IP_3, rather than a direct detergent-stable interaction between the two proteins.

Distinct localizations for two adaptor proteins

Tyrosine kinase cascades typically involve the phosphorylation and/or translocation of a series of tyrosine-phosphory-

Figure 2. **Actin and myosin are components of the cytoskeletal fibers that associate with membrane sheets, coprecipitate with PLCγ2, and contribute to PLCγ2 activation in suspension cells.** Membrane sheets were prepared from untreated RBL-2H3 cells and labeled with 5-nm antimyosin gold particles (A and B) and either 15- (B) or 5-nm (C) avidin-gold conjugated to biotinylated phalloidin to label filamentous actin. Arrowheads (A and B) point to examples of myosin label, typically found at branchpoints in the membrane-associated cytoskeletal meshwork. Arrows (B and C) point to examples of gold particles for actin that decorates, but does not uniformly label, the cytoskeletal cables. Coated vesicles (B and C) are marked (*). Bars, 0.1 μm. (D) PLCγ2 and myosin immune complexes were prepared from pooled fractions of sucrose density gradients, separated by SDS-PAGE, and probed for actin or PLCγ2.

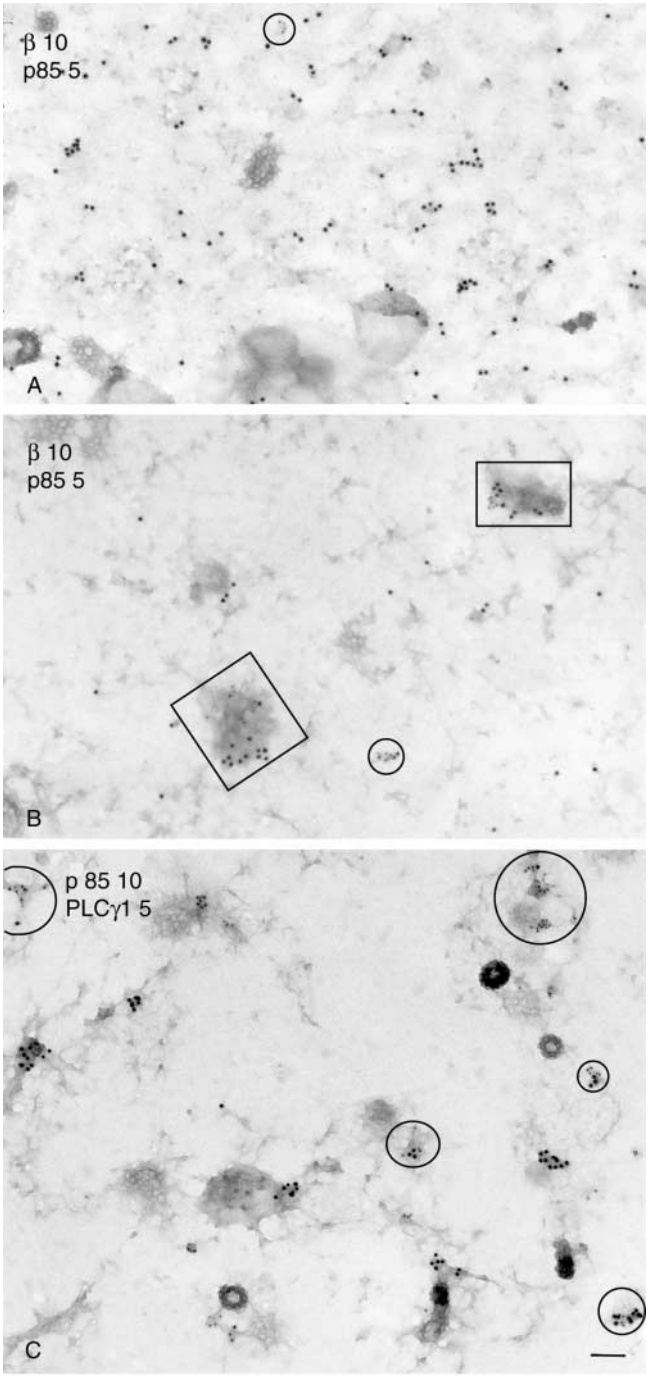

Figure 4. **PI3-kinase label colocalizes both with FcεRI in osmiophilic patches and with PLCγ1 outside of these patches in activated cells.** Membrane sheets were prepared from RBL-2H3 cells before (A) or after (B and C) FcεRI cross-linking. (A and B) The sheets were labeled with 5-nm anti-p85 gold particles and with 10-nm anti-FcεRI β gold particles. Resting cells have relatively little membrane-bound PI3-kinase (A, circled region). 5-nm gold particles marking p85 are strikingly colocalized with FcεRI β within the osmiophilic patches (boxed regions) of activated cells (B). (C) Sheets were labeled with 5-nm anti-PLCγ1 gold and 10-nm anti-p85 gold. PLCγ1 and p85 colocalize in activated cells in mixed clusters outside of osmiophilic patches (circled regions). Bar, 0.1 μm.

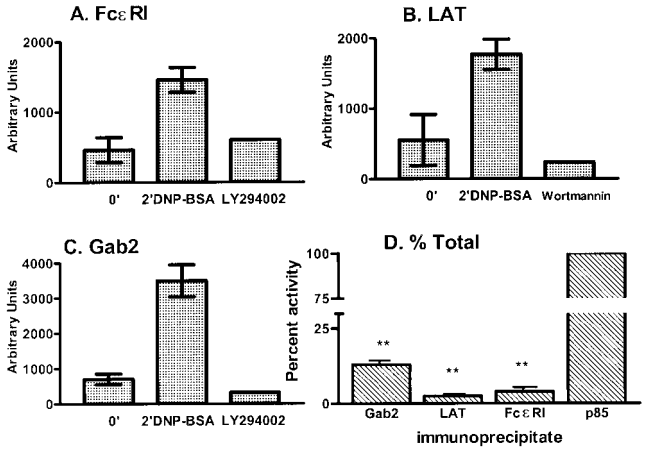

Figure 5. **Receptor cross-linking leads to increases in PI3-kinase activity associated with FcεRI, Gab2, and LAT.** Immune complexes were prepared from detergent lysates of RBL-2H3 cells before or after 2 min activation with DNP-BSA. To measure associated PI3-kinase activity, immune complexes were incubated with PtdIns and γ[^{32}P]ATP for 30 min at 37°C. Lipids in the reaction were extracted and resolved by TLC, and formation of PtdIns(3)P measured by PhosphorImager analysis. Background levels were established by adding PI3-kinase inhibitors (10 nM Wortmannin or 10 μM LY2940002) to replicate samples 15 min before initiating the reaction. As shown in A–C, there is an increase in PI3-kinase activity associated with FcεRI, Gab2, and LAT after 2 min of activation. Data are representative of at least three separate experiments, each performed in duplicate, and error bars represent SEM. Units are arbitary PhosphorImager values per 1,000. A one-sample *t* test was performed using Prism software (Graph Pad); all results have significant p-values (<0.03). (D) Shows the comparative levels of PI3-kinase activity in FcεRI, Gab2, and LAT precipitates, relative to total PI3-kinase activity in p85 immune complexes prepared from replicate lysates of antigen-stimulated cells. Data for Gab2 is from seven separate experiments (p-value = 0.00005); data for LAT (p-value = 0.0004) and FcεRI (p-value = 0.0288) are for three separate experiments.

lated adaptor proteins that serve as platforms for macromolecular assembly of downstream components. We hypothesized that PLCγ1 may be selectively segregated away from osmiophilic patches on membrane sheets from activated cells by its interaction with a scaffolding or adaptor protein. We selected Gab2 and LAT as candidates for analysis. Both of these proteins have been implicated in the coupling of receptor activation to changes in inositol phospholipid metabolism.

Grb2-associated binder 2 (Gab2) is a 100-kd cytoplasmic protein with a documented role in growth factor receptor coupling to PI3-kinase (Nishida et al., 1999). Results in Fig. 6 A show that Gab2 gold particles are relatively sparse on membrane sheets from resting cells. Nevertheless, a fraction of these gold particles (~18%) are in close proximity to FcεRI β (Table II). Gab2 gold label is increased 2.6-fold after FcεRI cross-linking. Furthermore, >50% of Gab2 is found in the FcεRI-, p85- and PLCγ2-containing osmiophilic patches that are induced by FcεRI cross-linking (Fig. 6 B; Table II).

We found recently that adhesion of RBL-2H3 cells leads to association of PI3-kinase with Gab2 (unpublished data; see Fig. 10 A). Despite this stable association, complementary biochemical assays showed that FcεRI cross-linking markedly increases PI3-kinase activity in anti-Gab2 immune complexes (Fig. 5 C), representing ~13% of total PI3-kinase activity (Fig. 5 D). These results suggest that p85 forms detergent-stable complexes with Gab2 that may localize active PI3-kinases to osmiophilic patches. Notably, because

Table II. **Gab2 distribution on membrane sheets**

	Resting	2′ XL
Total Gab2 particles	630	1663
Fold increase in Gab2 particles	—	2.6×
% colocalized with FcεRI β gold particles and in osmiophilic patches	18.5%	51%

Membrane sheets were prepared from IgE-primed resting or activated (2 min with 0.1 mg/ml DNP-BSA) cells and labeled for Gab2 and FcεRI β. Numbers of gold particles marking Gab2 and their proximity to particles marking FcεRI β were counted for 82.5 μm^2 of membrane.

FcεRI immunoprecipitates do not also contain Gab2 (data not shown), it is likely that the association of PI3-kinase with multiple proteins reflects redundant mechanisms to activate PI3-kinase.

LAT is an integral membrane protein whose cytoplasmic tail is palmitoylated and contains multiple tyrosine phosphorylation sites. LAT has been proposed to act as a scaffold for downstream signaling components and was recently shown to be a critical element upstream of PLCγ activation and calcium responses in antigen-stimulated mast cells (Saitoh et al., 2000; Kimura et al., 2001).

Counts of >10,000 LAT gold particles showed no differences in the density of LAT between membrane sheets from resting and cells that have stimulated for 2 min with antigen (data not shown). However, the organization of LAT is dramatically altered after short periods of FcεRI cross-linking. In Fig. 7 A, gold labeling for LAT identifies some singlets and numerous small clusters across membrane sheets prepared from unstimulated RBL-2H3 cells. In the majority of membrane sheets from resting cells, the number of gold particles per cluster is <20 (Fig. 8, A and B). Very few (<5%) of the 5-nm gold particles labeling LAT colocalize with 10-nm gold particles marking FcεRI β in unstimulated cells. Within 30 s of FcεRI cross-linking, very large elongated LAT clusters are found on membrane sheets (Fig. 7, B–E). Multiple groups of 50–150 gold particles were documented in cells activated for 30 s or 1 or 2 min (Fig. 8, B–E). LAT aggregates often transect the osmiophilic signaling patches that accumulate FcεRI β. However, rather than uniform mixing of the two sizes of gold label, they remain separate from each other. This is particularly evident in the large osmiophilic membrane patch seen in the upper left half of the micrograph in Fig. 7 B. Numerous LAT clusters are also found in apparently unspecialized membrane remote from aggregated FcεRI (Fig. 7, B and C).

Because PLCγ1 also redistributes on activated cells to membrane ruffles (Barker et al., 1998) and is dependent on D-3 phosphophoinositides for membrane recruitment, tyrosine phosphorylation and activation (Barker et al., 1998, 1999), it seemed likely that LAT might nucleate secondary signaling domains that include PLCγ1 and PI3-kinase. Analyses of membrane sheets double labeled for p85 and LAT support this hypothesis. Fig. 9 A shows the intersection, but not mixing, of large LAT clusters with p85 in a particularly dramatic osmiophilic patch after 2 min of antigen stimulation. There are also gold particles marking LAT away from the osmiophilic patches. These LAT clusters are larger than those on resting membranes and are strongly colocalized with p85 (Fig. 9 A, triangle regions).

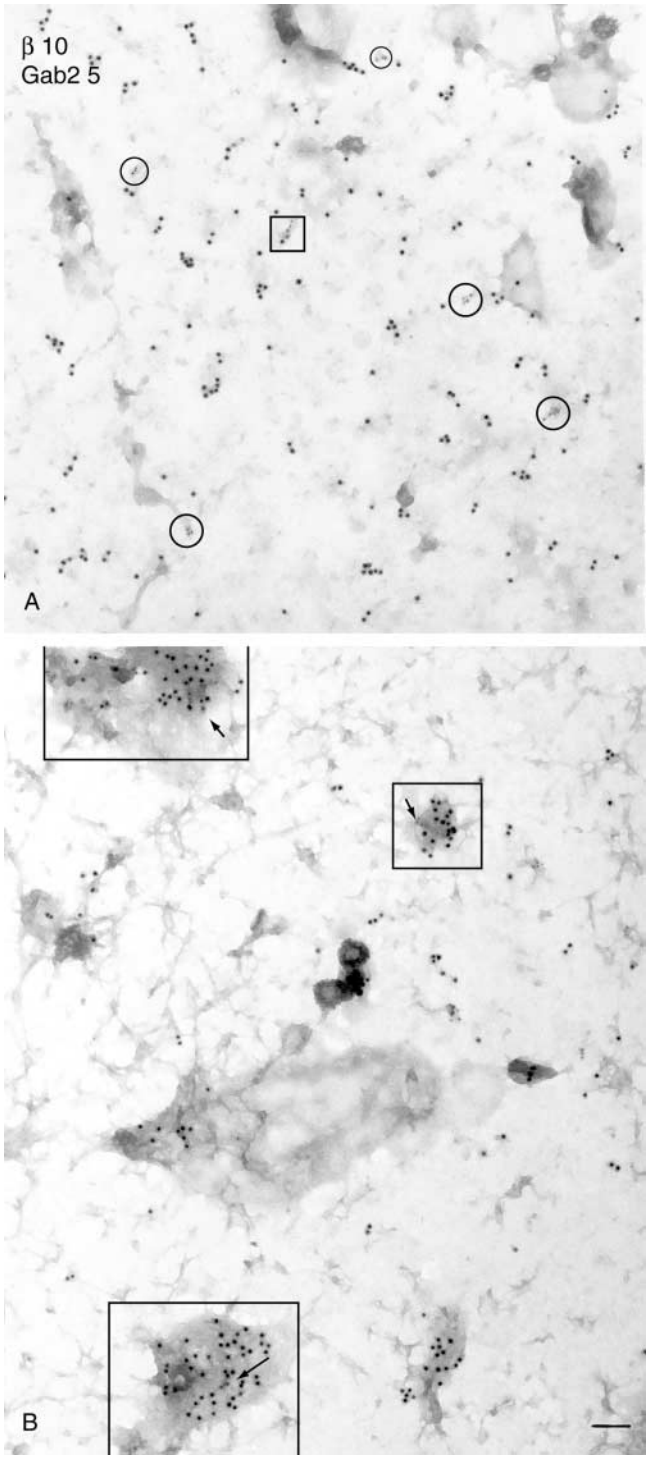

Figure 6. **Gab2 colocalizes with FcεRI in signaling patches in activated mast cells.** Membrane sheets were prepared from RBL-2H3 cells before (A) or after (B) cross-linking the FcεRI for 2 min with DNP-BSA. Membranes were labeled with 5-nm anti-Gab2 gold particles and with 10-nm anti-FcεRI β gold particles. (A) Shows that resting membranes have rather few 5-nm gold particles marking Gab2 (circled regions) and only occasional FcεRI β–Gab2 colocalization (boxed region). (B) Gold particles marking Gab2 (arrows) are strikingly colocalized with FcεRI β in osmiophilic patches of activated cells (boxed regions). Bar, 0.1 μm.

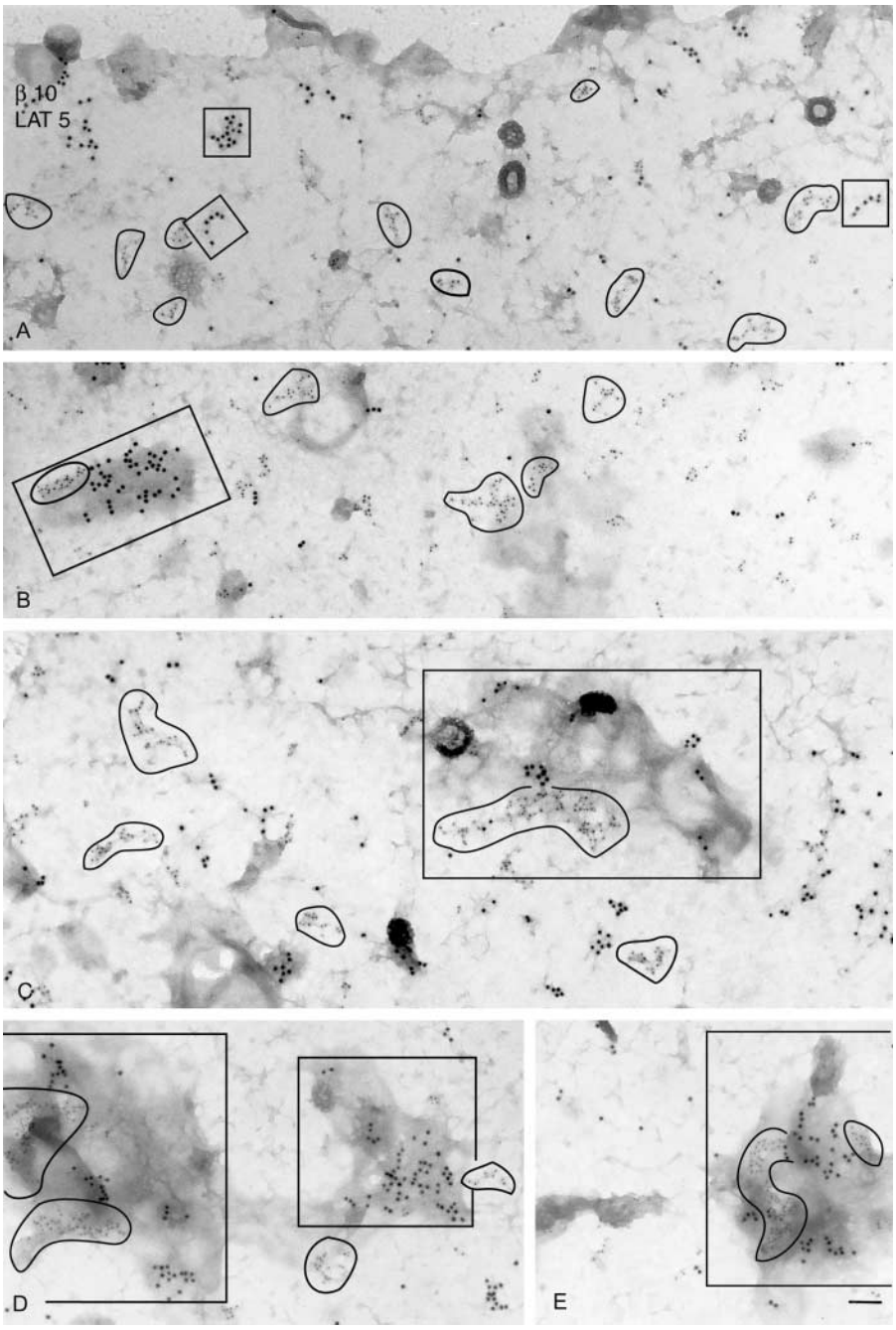

Figure 7. **LAT rafts are larger after FcεRI cross-linking and can intersect osmiophilic patches.** Membrane sheets prepared before (A) or after (B-E) cross-linking the FcεRI for 2 min with DNP-BSA were labeled with 5-nm gold particles for LAT and 10 nm gold particles for FcεRI β. (A) Shows that the numerous clusters of LAT (circled regions) and FcεRI (boxed regions) rarely colocalize in resting membranes. (B–E) Osmiophilic patches that label with FcεRI after 2 min activation are boxed and LAT clusters are outlined. LAT clusters in activated cells are often large (>50 particles). Bar, 0.1 μm.

Supporting the microscopy, anti-LAT immune complexes generated from RBL-2H3 cells coprecipitate the p85 subunit of PI3-kinase (Fig. 10 A). Although the amounts of p85 recovered in LAT precipitates is roughly equivalent in resting and antigen-stimulated cells, PI3-kinase activity is increased approximately threefold after FcεRI cross-linking (Fig. 5 B). Like FcεRI, the amount of PI3-kinase activity in LAT precipitates is a small but significant portion of the total activity measured in anti-p85 precipitates (Fig. 5 D). This may be an underestimate since coprecipitation of PI3-kinase with LAT is exceptionally sensitive to the detergent used during lysis. We found little PI3-kinase associated with LAT if immunoprecipitates were prepared from lysates solubilized in Brij 96 rather than Triton X-100 (not shown).

Importantly, PLCγ1 colocalizes with LAT after 2 min of FcεRI cross-linking. Gold particles marking PLCγ1 are frequently found at the edge of large LAT clusters (Fig. 9, B and C, arrowheads) and mixed with LAT in smaller clusters (Fig. 9, B–C, triangle regions). The inducible association of PLCγ1 with LAT inferred from microscopy of native membranes could also be demonstrated biochemically. Fig. 10 A shows a dramatic increase in PLCγ1 coprecipitating with anti-LAT immunoprecipitates from activated cells. Conversely, anti-PLCγ1 immunoprecipitates from activated but not resting cells contain coprecipitating LAT. Coprecipitation studies showed additionally that a portion of PLCγ2 also associates with LAT. However, the extent of PLCγ2-LAT coprecipitation was similar from both resting and activated cells, suggesting that PLCγ2 associates constitutively

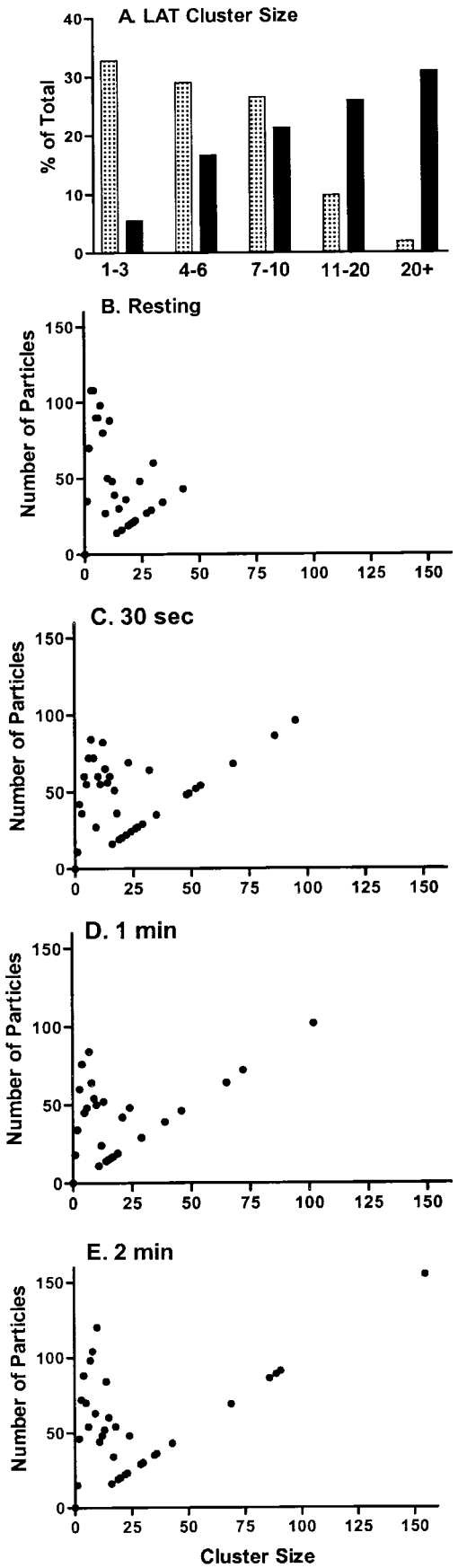

Figure 8. **FcεRI cross-linking leads to rapid increases in LAT cluster size.** (A) Summary data representing LAT cluster sizes in resting cells (hatched bars) or cells stimulated for 2 min with antigen (solid bars) for four independent experiments. A minimum of 3,000 gold particles were counted for each experimental condition. (B–E) Gold particles marking LAT were scored for cluster size in membrane sheets prepared from resting cells (B) or cells stimulated for 30 s (C), 1 min (D), or 2 min (E) with DNP-BSA. Counts are taken from one of two similar experiments.

with LAT (Fig. 10 A). (TEM confirmation of the inherent association of PLCγ2 with LAT was not obtained because the available antibodies to both molecules are rabbit polyclonals and thus unsuitable for double label studies.)

Biochemical analyses of isolated lipid rafts do not reproduce the protein interactions observed directly on native membrane sheets

Previous investigators have inferred properties of mast cell FcεRI signaling complexes from the composition of detergent-resistant membranes isolated by detergent extraction and sucrose density gradient centrifugation analysis of activated mast cells (Field et al., 1995, 1997, 1999; Surviladze, 1998). The results in Fig. 10 B reproduce published experiments showing that Lyn and LAT are both in the light fractions containing detergent-resistant membrane. A portion of FcεRI β is also recovered in these light fractions, with a modest increase seen in activated cells. This experiment is popularly interpreted as showing the activation-induced recruitment of cross-linked FcεRI to Lyn microdomains at the onset of signaling. However, it is difficult to reconcile with studies in native membranes showing that cross-linked FcεRI in fact segregate rapidly away from Lyn on native membranes (Wilson et al., 2000) and that receptor and LAT show little colocalization in resting cells and only transient colocalization in activated cells (this study).

The discrepancies are compounded when other signaling molecules are included in the analysis. A portion of PLCγ1 is redistributed to the detergent-resistant membrane, as might be expected if this membrane represents regions of active signaling. However, Syk is found separated from receptor in the heavy fractions of the sucrose gradient (Fig. 10 B). In contrast, Syk accumulates with cross-linked FcεRI in the osmiophilic patches of native membranes (Wilson et al., 2000). Similarly, Gab2, PLCγ isoforms, and PI3-kinase are all separated from both receptor and LAT in the heavy fractions of the gradient (Fig. 10 B), even though they can be found in close proximity to receptors and LAT in native membranes. In short, the results of sucrose gradient centrifugation analysis of detergent-extracted mast cells give a strikingly different impression of protein–protein interactions involved in FcεRI signaling than the impression obtained by direct microscopy on native membranes.

Discussion

We have used immunoelectron microscopy on native membrane sheets to map the topography of PLCγ1, PLCγ2, and the p85 subunit of PI3-kinase, all implicated in the remodeling of mast cell membrane inositol phospholipids in response to cross-linking the high-affinity IgE receptor, FcεRI. We have also examined the topography of the 38-kD transmembrane adaptor protein, LAT. LAT is a major substrate

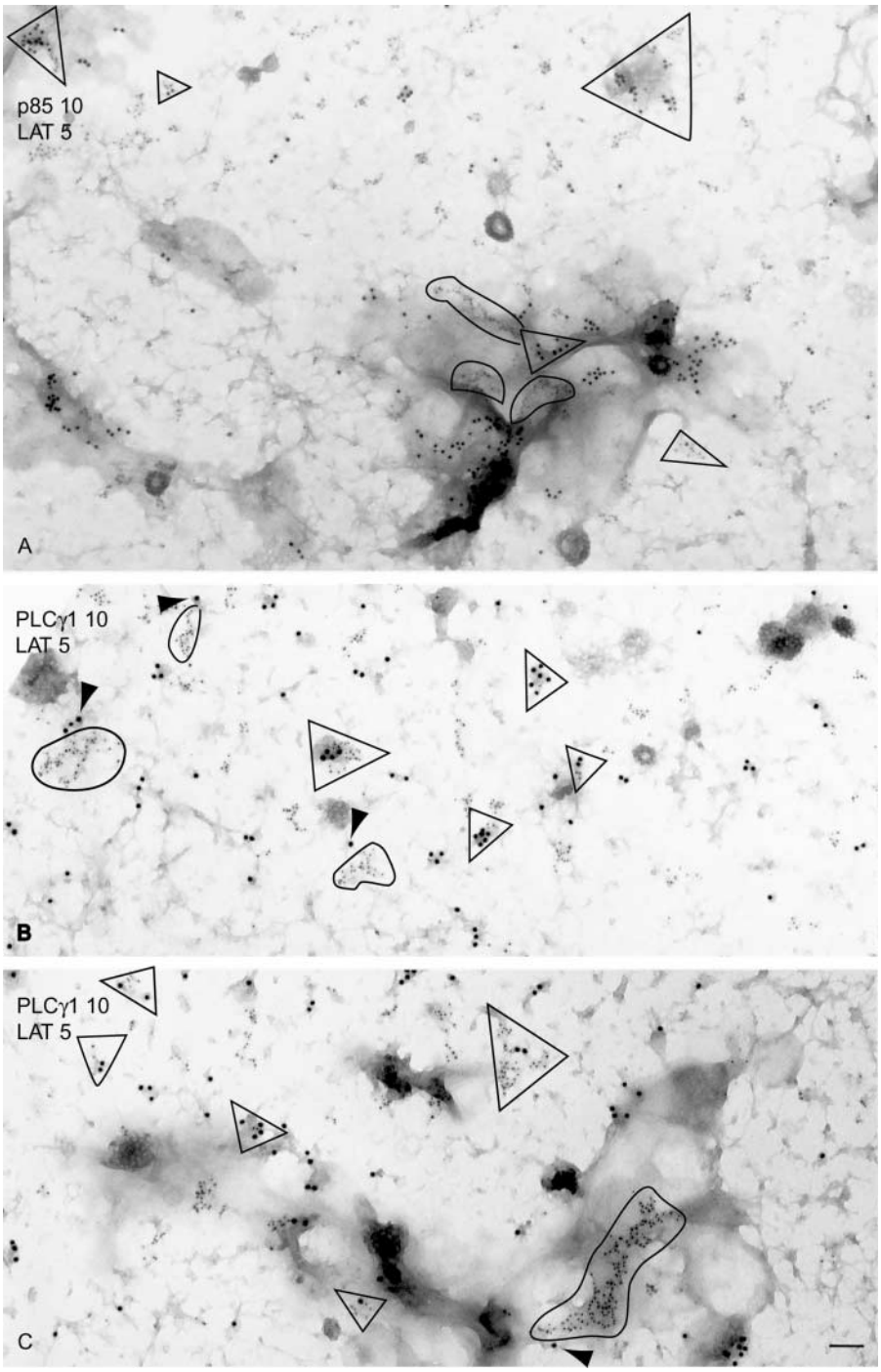

Figure 9. **LAT topography in relation to the distributions of PI3-kinase and PLCγ1.** Membrane sheets were prepared from antigen-stimulated RBL-2H3 cells and labeled with 5-nm anti-LAT gold particles (A–C) and with 10-nm gold particles specific for either the p85 regulatory subunit of PI3-kinase (A) or PLCγ1 (B and C). (A) Examples of LAT-PI3-kinase proximity are marked by triangles. Note that several large LAT rafts (circled regions) in an osmiophilic patch in the lower right do not mix extensively with nearby p85 clusters. (B and C) Examples of LAT-PLCγ1 colocalization are marked with triangles; separate LAT rafts are outlined. Note that colocalization is principally outside of osmiophilic patches. Bar, 0.1 μm.

of ZAP-70 and Syk (Weber et al., 1998; Zhang et al., 1998) that, in its phosphorylated form, mediates the SH2-dependent recruitment of several additional signaling molecules, including Grb2, Cbl, Vav, and PLCγ1. Finally, we have examined the topography of the adaptor protein, Gab2, during FcεRI signaling. Members of the Gab family of scaffolding proteins are tyrosine-phosphorylated in response to ligand binding to several growth factor and cytokine receptors (Holgado-Madruga et al., 1996; Gu et al., 1998; Nishida et al., 1999; Rodrigues et al., 2000; Schaeper et al., 2000; Gadina et al., 2000). We have recently found that Gab2 is the major tyrosine phosphorylated protein associated with class 1A PI3-kinases in antigen-stimulated adherent RBL-2H3 cells (unpublished data).

Previously, we demonstrated that cross-linked FcεRI encounter Syk in characteristic regions of the mast cell membrane that are easily identified by their dark staining with osmium and by the frequent formation of clathrin-coated pits at the periphery of the patch. Here, we show that the osmiophilic patches also accumulate PLCγ2, apparently reflecting a redistribution from its intrinsic associations in part with bulk membrane and in part with components of the cortical cytoskeleton. Osmiophilic patches also attract a substantial portion of class IA PI3-kinase heterodimers,

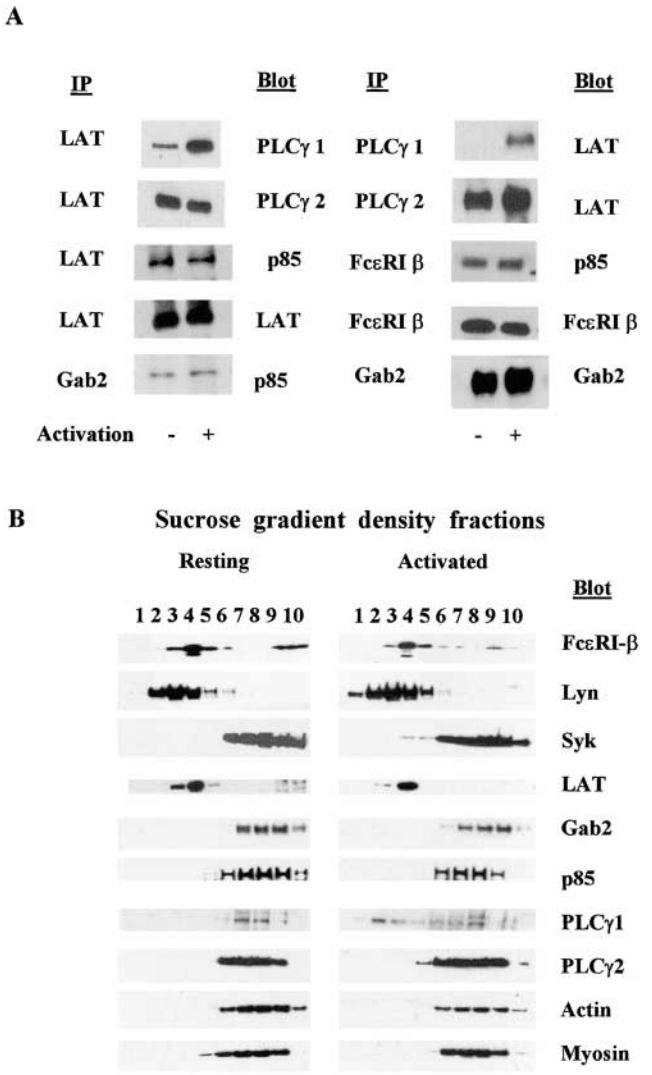

Figure 10. **Biochemical analyses of protein–protein interactions in activated mast cells.** (A) Coprecipitation studies demonstrate associations between signaling proteins. Resting and activated RBL-2H3 cells were solubilized in 0.5% Triton X-100, and the clarified cell lysates were used for immunoprecipitation afterwards by immunoblotting as indicated. Results show constitutive associations of p85 with LAT, Gab2, and FcεRI in adherent cells. They also show constitutive association of PLCγ2 with LAT and an inducible association of PLCγ1 with LAT. (B) Analysis of proteins distributed across sucrose density fractions. RBL-2H3 cells were solubilized in 0.05% Triton X-100 before (left) or after (right) cross-linking the FcεRI for 2 min with DNP-BSA. Cell lysates were loaded onto an 80% sucrose cushion, followed by layers of 35, 25, 20%, 15, and 10% sucrose. After ultracentrifugation, fractions were collected from the top (fraction 1) to the bottom of the gradient (from the lightest to heaviest fractions). Aliquots of the fractions were solubilized in Laemmli buffer, and proteins were resolved by SDS-PAGE, followed by immunoblot analysis as indicated in the key. Results show very little correlation with the protein–protein interactions observed by microscopy.

marked here by antibodies to the p85 regulatory subunit, that are translocated from the cytosol during mast cell activation. Additionally, these membrane patches recruit Gab2 that couples to Shc, Grb2, and SHP-2, as well as PI3-kinase (unpublished data). The accumulation of these signaling molecules further establishes the identity of the osmiophilic patches as sites of signaling from cross-linked FcεRI to downstream responses.

We show that FcεRI cross-linking also causes the formation of large elongated rafts that label with antibodies to the scaffolding protein, LAT. Although the LAT rafts often intersect osmiophilic patches containing FcεRI, they do not mix extensively with receptors in the patches. We hypothesize that the small LAT rafts characteristic of resting cells redistribute after FcεRI cross-linking into the osmiophilic patches, where they encounter and are phosphorylated by Syk. Modification of LAT may then promote the formation of larger, mobile LAT rafts. Our micrographs suggest that these rafts, which become prominent features outside of osmiophilic patches, may form separate domains for the docking of other proteins. At least two proteins are candidates for this docking activity: PLCγ1, whose association with LAT rafts is induced by FcεRI cross-linking (Fig. 10 A), and a portion of PI3-kinase that is apparently distinct from that associated with FcεRI or Gab2, based on coprecipitation studies (Fig. 5 B).

Several studies have implicated LAT, together with the SH2 domain–containing cytoplasmic adaptors in the SLP-76 family, in the activation of both PLCγ isoforms (Jevremovic et al., 1999; Pasquet et al., 1999; Ishiai et al., 2000; for reviews see Pivniouk and Geha, 2000; Myung et al., 2000). A direct association of LAT and PLCγ proteins is implied by coprecipitation studies (Fukazawa et al., 1995; Finco et al., 1998; Tridandapani et al., 2000; Martelli et al., 2000; Zhang et al., 2000) and by the isolation of LAT on immobilized PLCγ SH2(C) domains (Gross et al., 1999). Our results suggest different roles for LAT in the localization, and likely the activation, of the two PLCγ isoforms in mast cells. In RBL-2H3 cells, FcεRI cross-linking promotes the association of PLCγ1 with LAT domains, whereas a significant fraction of PLCγ2 appears to interact constitutively with LAT. Both results are consistent with previous evidence by immunogold labeling in thin section TEM that PLCγ1 is recruited to antigen-stimulated RBL membranes, whereas PLCγ2 is inherently at the membrane (Barker et al., 1998). The present results raise the possibility that PLCγ2 is inherently at the membrane as a result of its constitutive interaction with LAT and can redistribute to osmiophilic patches after FcεRI cross-linking. In contrast, PLCγ1 is transiently at the membrane when levels of D3-phosphoinositides produced by PI3-kinase in LAT domains are locally high.

We show that the topography of LAT on membrane sheets is markedly different from another class of adaptor, Gab2. Membrane-associated Gab2 was shown here to increase >2.5-fold in response to FcεRI cross-linking. Most of this Gab2 is found in the osmiophilic patches. Gab2 translocation is accompanied by a severalfold increase in associated PI3-kinase activity, identifying sites of Gab2 accumulation as potential sites of D-3 phosphoinositide synthesis.

Why would cells form multiple signaling domains? Because cross-linked FcεRI are internalized relatively rapidly by endocytosis through coated pits, whereas LAT is not internalized through coated pits, one prediction is that signaling domains organized by LAT may be more stable than signaling domains organized by FcεRI. In this case, one role for LAT domains could be to sustain and amplify signaling as

receptor levels drop. Interestingly, although secretion from RBL-2H3 cells halts within seconds of the addition of monovalent haptens that disrupt FcεRI aggregates, calcium levels remain high for several minutes (Lee and Oliver, 1995). This could be explained if LAT continues to serve as a scaffold for propagating signals to PI3-kinase and PLCγ proteins for some time after the disruption of FcεRI signaling patches. Another prediction is that distinct arms of the FcεRI signaling cascade could be propagated in these separate domains. These distinct arms may be complementary or, alternatively, may have independent outcomes.

Importantly, the p85 regulatory subunit of PI3-kinase can be found in both FcεRI and LAT domains. D-3 phosphoinositides represent a small and transient fraction of total membrane phosphoinositides (Traynor-Kaplan et al., 1989). Thus, the recruitment of PI3-kinase to specific domains may serve to generate the locally high concentrations of PtdIns(3,4,5)P_3 required for full activation of both PLCγ isoforms (Barker et al., 1999; Smith et al., 2001) at their distinct membrane locales (Barker et al., 1998). If this is true, then location is likely to be a factor in the activation of other enzymes, such as Akt, that also require PtdIns(3,4,5)P_3 or its metabolite PtdIns(3,4)P_2 for activation.

Many questions remain regarding the topography and functions of the class IA PI3-kinases. We showed previously that tyrosine phosphorylated proteins coprecipitate with all three p110 PI3-kinase catalytic subunits and that microinjection of blocking antibodies to the p110δ and p110β isoforms, but not p110α, inhibits calcium responses in RBL-2H3 cells (Smith et al., 2001). Here, we have observed that FcεRI cross-linking leads to increases in PI3-kinase activity in distinct macromolecular complexes organized around LAT, FcεRI, and Gab (Fig. 5). Together, these data raise the possibility that the different class IA PI3-kinases, composed of unique p85-p110 heterodimers, may distribute to distinct membrane domains to regulate different cellular functions. In particular, the presence of locally high PI3-kinase activity may induce locally high concentrations of D3-phosphoinositides to serve as lipid anchors for the recruitment of signaling molecules like PLCγ1. As well as determining the topography of recruited proteins, the local remodeling of membrane inositol phospholipid composition by nonrandomly distributed PI3-kinase family members may help to create or maintain preferred environments for transmembrane proteins like acylated LAT.

Current models of membrane structure envision membranes as dynamic mixtures of more or less ordered lipids in association with distinct proteins. An important example is the newly described immunological synapse that forms between the T cell and an antigen-presenting cell during conjugation of TCR–MHC peptide complexes (for review see Dustin and Chan, 2000). When observed by sophisticated fluorescence microscopic techniques, engaged TCR form the center of a bull's eye (referred to as the central supramolecular activation cluster or *cSMAC*), surrounded by a ring of adhesion receptors (the peripheral supramolecular activation cluster or *pSMAC*). Signaling molecules such as PKCθ may associate stably with the synapse (Monks et al., 1998), whereas others such as CD45 may be conditionally or transiently excluded (Sperling et al., 1998; Leupin et al., 2000; Johnson et al., 2000). Thus, the new models developed around data derived in both the TCR and FcεRI systems readily accommodate the concept that biological membranes may include one or more domains that are compositionally distinct from bulk membrane and can form and disassemble in a highly dynamic fashion. They also accommodate the hypothesis presented here that the segregation may be initiated in part when enzymes remodel the membrane inositol phospholipid composition after activation by receptor-coupled signaling pathways.

The relationship of the rafts isolated biochemically to the signaling domains observed microscopically remains to be determined. The protein associations we observe in native membrane sheets do not always correlate with implied associations based upon analysis of detergent-solubilized sucrose density fractions. For example, using the sucrose density fractionation protocol, we are able to confirm the localization of acylated proteins such as Lyn kinase and LAT to the light fraction. We also find a portion of PLCγ1 in the light fraction after FcεRI cross-linking. However, none of Syk, p85, PLCγ2, or Gab2 is found in the light fraction, even though their close interaction with receptor and LAT is readily demonstrated by TEM of native membranes.

In contrast, results using light microscopic approaches to elucidate interactions of FcεRI with rafts are more compatible with our results on native membrane sheets. Stauffer and Meyer (1997) showed that GFP chimeric proteins integrating the tandem SH2 domains of Syk were recruited to punctate structures at the plasma membrane, consistent with our observations that Syk is recruited to osmiophilic patches with receptors (Wilson et al., 2000). Using membrane sheets, we demonstrated that Lyn segregates from receptors with the first 2 min of cross-linking. The stringed appearance of Lyn as it segregates from osmiophilic patches, and the colocalization of Lyn with the actin-based cytoskeleton, suggests that cytoskeleton plays a role in Lyn's dissociation from receptors (Wilson et al., 2000). Using a complementary fluorescence confocal microscopy approach, Holowka et al. (2000) showed cytochalasin treatment leads to prolonged associations between cross-linked FcεRI and Lyn. Thus, a combination of light and electron microscopic approaches are likely to ultimately yield the clearest insight into the different protein–protein and protein–lipid interactions involved in the FcεRI signaling cascade.

Materials and methods

Reagents and cell culture

RBL-2H3 cells were grown in MEM (GIBCO BRL) supplemented with 10% fetal calf serum, penicillin–streptomycin, and L-glutamine. Monoclonal anti-p85α antibodies were from Santa Cruz Biotechnology, Inc. Rabbit anti-Gab2, anti-LAT and panreactive anti-p85 antibodies were from Upstate Biotechnology. Mouse anti-FcεRI β monoclonal antibodies and rabbit antimyosin (PTH) were gifts from Dr. Juan Rivera and Dr. Robert Adelstein, respectively (National Institutes of Health, Bethesda, MD). Anti-PLCγ1 (1249) and anti-PLCγ2 (Q-20) polyclonal antibodies were from Santa Cruz Biotechnology, Inc. Monoclonal antibodies to PLCγ1 were a mixture of E-12 (Santa Cruz Biotechnology, Inc.) and B-6-4 (Upstate Biotechnology). Isoform-specific PLCγ antibodies were tested by immunoblotting for absence of cross-reactivity to the other γ isoform. Affinity-purified mouse anti-DNP IgE was prepared as described (Liu et al., 1980; Seagrave et al., 1991). Anti–mouse HRP-conjugated antibodies were from Transduction Laboratories, and anti–rabbit HRP-conjugated antibodies were from Jack-

son ImmunoResearch Laboratories. Colloidal gold particles (5–10 nm in diameter) conjugated with anti–rabbit IgG, anti–mouse IgG, and streptavidin were from Nanoprobes and Amersham Pharmacia Biotech. Biotin–phalloidin and dinitrophenol-conjugated BSA (DNP-BSA) were from Molecular Probes.

Cell activation and membrane labeling

RBL-2H3 cells were allowed to settle overnight onto 15-mm round clean glass coverslips in the presence of anti-DNP IgE (1 μg/ml) to prime cell surface FcεRI. After washing to remove excess IgE, FcεRI were cross-linked by incubation for 2 min at 37°C with DNP-BSA (1 μg/ml). Plasma membrane sheets were prepared and labeled with antibody- or phalloidin-conjugated colloidal gold particles as described in Wilson et al. (2000), using a modification of procedures developed by Sanan and Anderson (1991). Samples were examined and photographed using an Hitachi H600 transmission electron microscope.

Quantifying gold particle distributions

Methods for counting gold particle distributions were established previously (Wilson et al., 2000). Here, micrographs from 2–4 separate experiments were sorted into groups according to distinct treatment and labeling conditions. For determination of cluster size and codistribution, gold particles were counted for matching sets of micrographs. Gold particles per set range 500–3,000 and reflect the relative abundance of label for antigen in the micrographs. For measuring translocation, numbers of gold particles were counted for each experimental condition over equivalent areas of membrane (defined in μm^2).

Sucrose gradient centrifugation and analysis of membrane fractions

IgE-primed RBL-2H3 cells (40×10^6 cells per treatment condition) were harvested from culture dishes with 1.5 mM EDTA in Hanks' buffered saline without divalent cations. Washed cells were resuspended in Hanks' buffered saline, divided into two aliquots, and held for 2 min at 37°C with or without DNP-BSA (1 μg/ml). Cells were collected by centrifugation at 4°C, cell pellets were resuspended in 750 μl ice-cold lysis buffer containing low concentrations of detergent (10 mM Tris/HCl, pH 8.0, 0.05% Triton X-100, 50 mM NaCl, 10 mM EDTA, 10 mM glycerophosphate, 1 mM $NaV0_4$ and 1× protease inhibitor cocktail from Roche Molecular Chemicals). Lysates were mixed with 750 μl 80% sucrose (prepared in 10 mM Tris-HCl, pH 8.5, 50 mM NaCl, 2 mM EDTA) and overlaid onto 0.5 ml 80% sucrose in polyallomer tubes (13 × 51 mm), followed by 0.5-ml layers of 35, 25, and 20% and 0.6-ml aliquots of 15 and 10%. The gradient was centrifuged in a SW 55 (Beckman) rotor at 200,000 *g* for 16 h at 4°C. Fractions (0.5 ml) were harvested sequentially from the top of the gradient. For analyses of protein composition, aliquots (35 μl) were mixed with equal volume of 2× SDS sample buffer, boiled for 5 min, and separated by 8 or 10% SDS-PAGE. Alternatively, designated fractions were diluted in 50 mM Tris, 150 mM NaCl, pH 7.4, 1 mM $NaV0_4$ to a total volume of 1 ml and rocked for 1 h with beads prebound to primary antibodies, followed by separation of proteins bound to washed beads by SDS-PAGE. Proteins were transferred to nitrocellulose using a semidry blotting system (Labconco). Blots were probed with primary antibodies (1 μg/ml), followed by HRP-conjugated secondary antibodies (anti–mouse HRP-conjugates were diluted 1:10,000, and anti–rabbit HRP-conjugates were diluted 1:40,000); immunolabeled proteins were visualized by fluorography (ECL, Pierce Chemical Co.).

PI3-kinase assays

IgE-primed RBL cells were incubated with or without DNP-BSA at 37°C, and reactions were stopped with ice-cold saline. Cells were sedimented by microcentrifugation and lysed in 50 mM Tris/HCl, pH 7.2, 150 mM NaCl, 1 mM $NaV0_4$, and protease inhibitor cocktail (Boehringer) containing 1% Brij 96 or 1% Triton X-100, as specified. Lysates were clarified by centrifugation (15,000 *g*) for 5 min and rocked 2 h at 4°C with 40 μl (per ml of lysate) protein A– and G–Sepharose bead mixture (1:1) (Amersham Pharmacia Biotech) prebound to specified antibodies (1 μg). Washed immune complexes were incubated in reaction buffer (20 mM Hepes, pH 7.4, 5 mM $MgCl_2$, 0.25 mM EGTA), containing 10 μM ATP, 20 μCi $\gamma[^{32}P]$ATP, 500 μg/ml sonicated PtdIns (50 μl total) for 30 min at 37°C. The reactions were stopped by addition of 3N HCl. The lipid fraction was isolated using chloroform–methanol partitioning (Jackson et al., 1992) and resolved by thin-layer chromatography in 1-propyl acetate:2-propanol:ethanol:6% aqueous ammonia (1:3:1:3) (vol/vol) on silica gel 60 plates (Merck) (Hegewald, 1996). Formation of ^{32}P-labeled PtdIns(3)P was imaged on a STORM 860 PhosphorImager (Molecular Dynamics) and quantified by means of Image Quant software. Data shown are duplicates ± SEM and are representative of at least three experiments.

Use of the electron microscopy facility at the University of New Mexico School of Medicine is gratefully acknowledged.

This work was supported in part by American Cancer Society grant RPG-99-233-01-CIM to B.S. Wilson and by National Institutes of Health grant RO1 GM49814 to J.M. Oliver.

Submitted: 12 April 2001
Revised: 27 June 2001
Accepted: 2 July 2001

References

Anderson, R.G.W. 1998. The caveolae membrane system. *Ann. Rev. Biochem.* 67: 199–225.

Barker, S.A., K.K. Caldwell, J.R. Pfeiffer, and B.S. Wilson. 1998. Wortmannin-sensitive phosphorylation, translocation and activation of PLCγ1, but not PLCγ2, in antigen-stimulated RBL-2H3 mast cells. *Mol. Biol. Cell.* 9:483–496.

Barker, S.A., D. Lujan, and B.S. Wilson. 1999. Multiple roles for PI3-kinase in the regulation of PLCγ activity and Ca^{2+} mobilization in antigen-stimulated mast cells. *J. Leukoc. Biol.* 65:321–329.

Berlin, R.D., J.M. Oliver, T.E. Ukena, and H.H. Yin. 1974. Control of cell surface topography. *Nature.* 247:45–46.

Berlin, R.D., J.M. Oliver, T.E. Ukena, and H.H. Yin. 1975. The cell surface. *New Engl. J. Med.* 292:515–520.

Brown, D.A., and E. London. 1998. Functions of lipid rafts in biological membranes. *Ann. Rev. Cell Dev. Biol.* 14:111–136.

Dráber, P., L. Dráberová, M. Kovárová, I. Hálová, H. Pavel, M. Erná, and R.K. Boubel. 2001. Lipid rafts and their role in signal transduction—mast cells as a model. *Trends Glycosci. Glyc.* In press.

Dustin, M.L., and A.C. Chan. 2000. Signaling takes shape in the immune system. *Cell.* 103:283–294.

Edidin, M. 1997. Lipid microdomains in cell-surface membranes. *Curr. Opin. Struct. Biol. 7*:528–532.

Field, K.A., D. Holowka, and B. Baird. 1995. FcεRI-mediated recruitment of p53/56^{lyn} to detergent-resistant membrane domains accompanies cellular signaling. *Proc. Natl. Acad. Sci. USA.* 92:9201–9205.

Field, K.A., D. Holowka, and B. Baird. 1997. Compartmentalized activation of the high affinity immunoglobulin E receptor within membrane domains. *J. Biol. Chem.* 272:4276–4280.

Field, K.A., D. Holowka, and B. Baird. 1999. Structural aspects of the association of FcεRI with detergent-resistant membranes. *J. Biol. Chem.* 274:1753–1758.

Finco, T.S., T. Kadlecek, W. Zhange, L.E. Samelson, and A. Weiss. 1998. LAT is required for TCR-mediated activation of PLCγ1 and the Ras pathway. *Immunity.* 9:617–626.

Fukazawa, T., K.A. Reedquist, G. Panchamoorthy, S. Soltoff, T. Trub, B. Bruker, L. Cantley, S.E. Shoelson, and H. Band. 1995. T cell activation-dependent association between the p85 subunit of the phosphatidylinositol 3-kinase and Grb2/phospholipase C-γ1-binding phosphotyrosyl protein pp36/38. *J. Biol. Chem.* 270:20177–20182.

Gadina, M., C. Sudarshan, R. Visconti, Y.J. Zhou, H. Gu, B.G. Neel, and J.J. O'Shea. 2000. The docking molecule Gab2 is induced by lymphocyte activation and is involved in signaling by interleukin-2 and interleukin-15 but not other common γ chain-using cytokines. *J. Biol. Chem.* 275:26959–26966.

Gross, B.S., S.K. Melford, and S.P. Watson. 1999. Evidence that phospholipase C-γ2 interacts with SLP-76, Syk, Lyn, LAT and the Fc receptor γ-chain after stimulation of the collagen receptor glycoprotein VI in human platelets. *Eur. J. Biochem.* 263:612–623.

Gu, H., J.C. Pratt, S.J. Burakoff, and B.G. Neel. 1998. Cloning of p97/Gab2, the major SHP-2 binding protein in hematopoietic cells, reveals a novel pathway for cytokine-induced gene activation. *Mol. Cell.* 2:729–740.

Hegewald, H. 1996. One-dimensional thin-layer chromatography of all known D-3 and D-4 isomers of phosphoinositides. *Anal. Biochem.* 242:152–155.

Holowka, D., E.D. Sheets, and B. Baird. 2000. Interactions between FcεRI and lipid raft components are regulated by the actin cytoskeleton. *J. Cell Sci.* 113:1009–1019.

Holgado-Madruga, M., D.R. Emlet, D.K. Moscatello, A.K. Godwin, and A.J.

Wong. 1996. A Grb2-associated docking protein in EGF- and insulin-receptor signalling. *Nature.* 379:560–564.

Horejsi, V., K. Drbal, M. Cebecauer, J. Cerny, T. Brdicka, P. Angelisova, and H. Stockinger. 1999. GPI-microdomains: a role in signalling via immunoreceptors. *Immunol. Today.* 20:356–361.

Ishiai, M., M. Kurosaki, K. Inabe, A.C. Chan, K. Sugamura, and T. Kurosaki. 2000. Involvement of LAT, Gads and Grb2 in compartmentation of SLP-76 to the plasma membrane. *J. Exp. Med.* 192:847–856.

Jacobson, K., and C. Dietrich. 1999. Looking at lipid rafts? *Trends Cell Biol.* 9:87–91.

Jackson, T.R., L.R. Stephens, and P.T. Hawkins. 1992. Receptor specificity of growth factor-stimulated synthesis of 3-phosphorylated inositol lipids in Swiss 3T3 cells. *J. Biol. Chem.* 267:16627–16636.

Jevremovic, D., D.D. Billadeau, R.A. Schoon, C.J. Dick, B.J. Irvin, W. Zhang, L.E. Samelson, R.T. Abraham, and P.J. Leibson. 1999. A role for the adaptor protein LAT in human NK cell-mediated cytotoxicity. *J. Immunol.* 162: 2453–2456.

Johnson, K., S.K. Gomley, M.L. Dustin, and M.L. Thomas. 2000. A supramolecular basis for CD45 regulation during T cell activation. *Proc. Natl. Acad. Sci. USA.* 97:10138–10143.

Kimura, T., M. Hisano, Y. Inoue, and M. Adachi. 2001. Tyrosine phosphorylation of the linker for activator of T cells in mast cells by stimulation with the high affinity IgE receptor. *Immunol. Lett.* 75:123–129.

Langlet, C., A.-M. Bernard, P. Drevot, and H.-T. He. 2000. Membrane rafts and signaling by the multichain immune recognition receptor. *Curr. Opin. Immunol.* 12:250–255.

Lee, R.J., and J.M. Oliver. 1995. Roles for Ca^{2+} stores release and two Ca^{2+} influx pathways in the FcεRI-activated Ca^{2+} responses of RBL-2H3 cells. *Mol. Biol. Cell.* 6:825–839.

Leupin, O., R. Zaru, T. Laroche, S. Muller, and W. Valitutti. 2000. Exclusion of CD45 from the T-cell receptor signaling area in antigen-stimulated T lymphocytes. *Curr. Biol.* 10:277–280.

Liu, F.T., J.W. Bohn, E.L. Ferry, H. Yamamoto, C.A. Molinaro, L.A. Sherman, N.R. Klinman, and D.H. Katz. 1980. Monoclonal dintrophenyl-specific murine IgE antibody: preparation, isolation and characterization. *J. Immunol.* 24:2728–2737.

Martelli, M.P., H. Lin, W. Zhang, L.E. Samelson, and B.E. Bierer. 2000. Signaling via LAT (linker for T-cell activation) and Syk/ZAP-70 is required for ERK activation and NFAT transcriptional activation following CD2 stimulation. *Blood.* 96:2181–2190.

Monks, C.R., B.A. Breiberg, H. Kupfer, N. Sciaky, and A. Kupfer. 1998. Three-dimensional segregation of supramolecular activation in T cells. *Nature.* 395:82–86.

Myung, P.S., N.J. Boerthe, and G.A. Koretzky. 2000. Adaptor proteins in lymphocyte antigen-receptor signaling. *Curr. Opin. Immunol.* 12:256–266.

Nishida, K., Y. Yoshida, M. Itoh, T. Fukada, T. Ohtani, T. Shirogane, T. Atsumi, M. Takahashi-Tezuka, K. Ishihara, M. Hibi, and T. Hirano. 1999. Gab-family adapter proteins act downstream of cytokine and growth factor receptors and T- and B-cell antigen receptors. *Blood.* 93:1809–1816.

Oliver, J.M., T.E. Ukena, and R.D. Berlin. 1974. Effects of phagocytosis and colchicine on the distribution of lectin-binding sites on cell surfaces. *Proc. Nat. Acad. Sci. USA.* 71:394–398.

Pasquet J.-M., B. Gross, L. Quek, N. Asazuma, W. Zhang, C.L. Sommers, E. Schweighoffer, V. Tybulewicz, B. Judd, J.R. Lee, G. Koretzky, P.E. Love, L.E. Samelson, and S.P. Watson. 1999. LAT is required for tyrosine phosphorylation of phospholipase Cγ2 and platelet activity by the collagen receptor GPVI. *Mol. Cell. Biol.* 19:8326–8334.

Pivniouk, V.I., and R.S. Geha. 2000. The role of SLP-76 and LAT in lymphocyte development. *Curr. Opin. Immunol.* 12:173–178.

Rodrigues, G.A., M. Falasca, Z. Zhang, S.H. Ong, and J. Schlessinger. 2000. A novel positive feedback loop mediated by the docking protein Gab1 and phosphatidylinositol 3-kinase in epidermal growth factor receptor signaling. *Mol. Cell. Biol.* 20:1448–1459.

Saitoh, S., R. Arudchandran, T.S. Manetz, W. Zhang, C.L. Sommers, P.E. Love, J. Rivera, and L.E. Samelson. 2000. LAT is essential for FcεRI-mediated mast cell activation. *Immunity.* 12:525–535.

Sanan, D.A., and R.G.W. Anderson. 1991. Simultaneous visualization of LDL receptor distribution and clathrin lattices on membranes torn from the upper surface of cultured cells. *J. Histochem. Cytochem.* 39:1017–1024.

Schaeper, U., N.H. Gehring, K.P. Fuchs, M. Sachs, B. Kempkes, and W. Birchmeier. 2000. Coupling of Gab1 to c-Met, Grb2, and Shp2 mediates biological responses. *J. Cell Biol.* 149:1419–1432.

Seagrave, J.C., J.R. Pfeiffer, C. Wofsy, and J.M. Oliver. 1991. The relationship of IgE receptor topography to secretion in RBL-2H3 mast cells. *J. Cell Phys.* 148:139–151.

Simons, K., and E. Ikonen. 1997. Functional rafts in cell membranes. *Nature.* 387: 569–572.

Singer, S.J., and G.L. Nicolson. 1972. The fluid mosaic model of the structure of cell membranes. *Science.* 175:720–731.

Smith, A.J., Z. Surviladze, E.A. Gaudet, J.M. Backer, C.A. Mitchell, and B.S. Wilson. 2001. p110β and p110δ PI-3 kinases upregulate FcεRI-activated Ca^{2+} influx by enhancing IP_3 production. *J. Biol. Chem.* In press.

Sperling, A.I., J.F. Sedy, H. Manjunath, A Kupfer, B. Ardman, and J.K. Burkdardt. 1998. TCR signaling induces selective exclusion of CD43 from the T cell-antigen-presenting cell contact site. *J. Immunol.* 161:6459–6462.

Stauffer, T.P., and T. Meyer. 1997. Compartmentalized IgE receptor-mediated signal transduction in living cells. *J. Cell Biol.* 139:1447–1454.

Surviladze, A., L. Dráberová, L. Kubinová, and P. Dráber. 1998. Functional heterogeneity of Thy-1 membrane microdomains in rat basophilic leukemia cells. *Eur. J. Immunol.* 28:1847–1858.

Teruel, M.N., and T. Meyer. 2000. Translocation and reversible localization of signaling proteins: a dynamic future for signal transduction. *Cell.* 103:181–184.

Traynor-Kaplan, A.E., B.L. Thompson, A.L. Harris, P. Taylor, G.M. Omann, and L.A. Sklar. 1989. Transient increase in phosphatidylinositol 3,4-bisphosphate and phosphatidylinositol trisphosphate during activation of human neutrophils. *J. Biol. Chem.* 264:15668–15673.

Tridandapani, S., T.W. Lyden, J.L. Smith, J.E. Carter, K.M. Coggeshall, and C.L. Anderson. 2000. The adaptor protein LAT enhances Fcγ receptor-mediated signal transduction in myeloid cells. *J. Biol. Chem.* 275:20480–20487.

Tsan, M.F., and R.D. Berlin. 1971. Effect of phagocytosis on membrane transport of non-electrolytes. *J. Exp. Med.* 134:1016–1035.

Weber, J.R., S. Orstavik, K.M. Torgersen, N.C. Danbolt, S.F. Berg, J.C. Ryan, K. Tasken, J.B. Imboden, and J.T. Vaage. 1998. Molecular cloning of the cDNA encoding pp36: a tyrosine phosphorylated adaptor protein selectively expressed by T cells and natural killer cells. *J. Exp. Med.* 187:1157–1161.

Wilson, B.S., J.R. Pfeiffer, and J.M. Oliver. 2000. Observing FcεRI signaling from the inside of the mast cell membrane. *J. Cell Biol.* 149:1131–1142.

Zhang, W., R.P. Trible, and L.E. Samelson. 1998. LAT palmitoylation: its essential role in membrane microdomain targeting and tyrosine phosphorylation during T cell activation. *Immunity.* 9:239–246.

Zhang, W., R.P. Trible, M. Zhu, S.K. Liu, C.J. McGlade, and L.E. Samuelson. 2000. Association of Grb2, Gads, and phospholipase C-γ1 with phosphorylated LAT tyrosine residues. *J. Biol. Chem.* 275:23344–23361.